ELSEVIER

Journal of Molecular Catalysis A: Chemical 153 (2000) 257–266

JOURNAL OF MOLECULAR CATALYSIS A: CHEMICAL

www.elsevier.com/locate/molcata

The gas phase hydrogenation of 2-butanone over supported nickel catalysts: introduction of enantioselectivity

Amalia López-Martínez, Mark A. Keane *

Department of Chemical Engineering, The University of Leeds, Leeds, LS2 9JT, UK

Received 2 June 1999; accepted 13 September 1999

Abstract

The gas phase hydrogenation of 2-butanone to 2-butanol at 343 K promoted using a Y zeolite-supported nickel catalyst (2.2% w/w Ni) prepared by ion exchange and a range of Ni/SiO_2 catalysts (1.5–20.3% w/w Ni) prepared by precipitation/deposition and impregnation has been studied. The freshly activated catalysts generated racemic products and enantioselectivity was introduced to a negligible degree by in situ and to an appreciable degree by ex situ treatment with a methanolic solution of L-tartaric acid. The effectiveness of the latter modification was strongly dependent on modifier concentration and an optimum enantiomeric excess (ee) of 31% was achieved at an intermediate tartaric acid concentration (8×10^{-3} mol dm^{-3}) where the latter also served to raise the fractional conversion of the 2-butanone feedstock when compared with the unmodified catalyst under the same reaction conditions. Treatment with L-valine or L-glutamic acid did not result in the introduction of any appreciable level of product optical activity. Conversion of 2-butanone over Ni/SiO_2 was subject to a short term loss of catalytic activity which was however readily restored by heating in flowing hydrogen at 673 K. Deactivation of the Ni/Na-Y catalyst was more severe and was not reversed by such a heat treatment; loss of activity in this case is attributed to an irreversible pore blocking. Non-selective hydrogenation is approximated by pseudo-first-order kinetics, the possibility of thermodynamic limitations is considered and the effects of varying the hydrogen partial pressure and gas space velocity are addressed. The reaction exhibits a high degree of structure sensitivity and the relationship between specific rate constant and nickel particle diameter is presented wherein an optimum particle size of ca. 3 nm is identified.

Keywords: Hydrogenation; 2-Butanone; Enantioselectivity; Structure sensitivity; Nickel/silica; Nickel/zeolite Y

1. Introduction

A large proportion of the chemicals used in the production of pharmaceuticals and pesticides contain at least one chiral centre [1]. The synthesis of enantiomerically pure chiral compounds is accordingly important on a commercial scale, particularly in the pharmaceutical, agrochemical and flavours/fragrances industries [2]. Possible synthetic routes to chiral production include the use of chiral pools [1], resolution of racemates [3] or asymmetric synthesis [4]. The latter possibility typically involves some form of enzyme or synthetic catalyst to promote the enantioselective step. Enzymatic systems are characterised by high reaction rates and optical yields but a very narrow band of optimum process conditions

* Corresponding author. Tel.: +44-113-233-2428; fax: +44-113-233-2405.

E-mail address: chemaak@leeds.ac.uk (M.A. Keane).

1381-1169/00/$ - see front matter
PII: S1381-1169(99)00356-8

where reaction temperatures in excess of 363 K normally results in a denaturation of the native structure [5] and loss of activity. In contrast to enzymes, few synthetic catalysts exhibit exclusive reaction selectivity and will promote a variety of reactions. Many homogeneous chiral catalyst systems employing transition metals are now well-established [6]. Conventional supported catalysts possess no inherent chirality and must be treated with an optically active modifier in order to induce some degree of enantiodifferentiation. The viability of heterogeneous enantioselective catalysts has yet to be fully explored and the research to date has largely focused on two systems [7,8], namely the asymmetric hydrogenation of hydrogenation of ethyl pyruvate and methyl acetoacetate using cinchonidine-modified platinum and tartaric acid-modified nickel catalysts, respectively. At present, the large-scale production of enantiomers is achieved via resolution (diastereoisomeric/enzymatic) or asymmetric synthesis where both batch processes are multi-stepped, involving costly enantiomeric reagents with coproduct impurities that can require additional and involved separation steps. The development of a highly selective solid catalyst that operates in a gas phase continuous reaction mode certainly represents a cleaner route to a single-enantiomeric product.

In this paper we examine the gas phase hydrogenation of 2-butanone to 2-butanol where the latter exists in two enantiomeric forms. The reaction was chosen as a simple model system principally because of the moderate temperatures needed to ensure gas phase conditions. The non-selective hydrogenation of 2-butanone has been reported for a homogeneous liquid phase application using various ruthenium complexes [9], an heterogeneous liquid phase system emplying Rh–Sn/SiO_2 [10] and in the gas phase over MgO [11]. We consider, in the first instance, the racemic conversion of 2-butanone over a range of unpromoted nickel catalysts before examining the effect of in situ and ex situ modification with three selected optically active reagents, i.e., L-tartaric acid, L-valine and L-glutamic acid. Previous studies of tartaric acid [12–14] and alanine [15,16] treatments of silica-supported nickel systems have revealed the interrelated nature of the variables involved in the modification process where changes in the modification time and temperature, modifier concentration, modifier pH and modification medium all have a bearing on the ultimate active phase and the observed activities/selectivities. The enantioselective hydrogenation of 2-butanone is not a well-studied reaction and a search through the BIDS Compendex (1974–1999), the BIDS ISI (1981–1999) and a review of the older literature only unearthed three reports [17–19] that described the application of tartaric acid-modified Raney nickel. In each case, the reaction was conducted in the liquid phase and the highest achieved optical yield (72%) was appreciably greater than that (48%) recorded for an enzymatic (alcohol dehydrogenase) system [20]. We provide herein preliminary gas phase enantioselectivity data for modified supported nickel systems.

2. Experimental

2.1. Catalyst preparation and activation

Five silica-supported nickel catalysts of varying metal loading (in the range of 1.5–20.3% w/w Ni) were prepared by homogeneous precipitation/deposition [21] and the catalytic action of each was compared with an 11.6% w/w Ni/SiO_2 prepared by impregnation [22] and a 2.2% w/w Ni–Na/Y zeolite prepared by ion exchange [23]. The hydrated samples, sieved in the 150–200 μm mesh range, were activated by heating in a 100-cm^3 min^{-1} stream (monitored using a Humonics Model 529 digital flow meter) of dry hydrogen (99.9%) at a fixed rate of 5 K min^{-1} (controlled using a Eurotherm 91e temperature programmer) to a final temperature of 673 ± 1 K which was maintained for 18 h.

Nickel metal dispersion/particle size was evaluated by CO chemisorption, TEM and XRD line broadening as described previously [21,22].

2.2. Modification with optically active reagents

2.2.1. In situ modification

All the catalyst precursor activation and 2-butanone hydrogenation steps were carried out under atmospheric pressure in a fixed bed continuous flow glass reactor (i.d. = 15 mm) that satisfactorily approximated plug flow pattern [24]. The catalyst was supported on a glass frit and a layer of glass beads above the catalyst bed ensured that all modifiers/reactant reached the modification/reaction temperature before contacting the catalyst. The reactor temperature was monitored by a thermocouple inserted in a thermowell within the catalyst bed; reactor temperature was constant to within ± 1 K. After the reduction step, the catalyst bed temperature was lowered to 343 K and a Model 100 (kd Scientific) microprocessor controlled infusion pump was used to deliver saturated methanolic solutions of L-valine (Aldrich, 99%) and L-glutamic acid (Aldrich, 99%) and a 0.2 mol dm^{-3} methanolic solution of L-tartaric acid (Aldrich, 99.5%) via a glass/Teflon air-tight syringe and teflon line at a fixed rate of 0.03 cm^3 min^{-1} for 1 h. The vapour was carried through the catalyst bed in a 100 cm^3 min^{-1} stream of purified helium. The catalyst was then flushed in flowing hydrogen (100 cm^3 min^{-1}) for 1 h at 343 K before introducing the 2-butanone reactant.

2.3. Ex situ modification

The catalyst precursor was activated as above, cooled in helium to room temperature, contacted with anhydrous methanol (Aldrich, 99.9 + %) and transferred to a 100-cm^3 methanolic solution of L-tartaric acid where the modifier concentration was in the overall range of 4×10^{-3}–16×10^{-3} mol dm^{-3}. Modification was performed, where $T = 293 \pm 2$ K, at a constant stirring speed of 600 rpm for 1 h. After modification, the catalyst was decanted and washed with 2×25 cm^3 methanol, dried at 343 K and reloaded into the catalytic reactor where the catalyst was contacted with 100 cm^3 min^{-1} dry hydrogen for 1 h before introducing the 2-butanone reactant. The post-modification solution was analysed by HPLC to ascertain the concentration of tartaric acid adsorbed and by atomic absorption spectrophotometry to monitor the extent of nickel leaching from the catalyst: the procedures used have been described in some detail in previous reports [14,16].

2.4. Catalytic procedure

Undiluted 2-butanone (Aldrich, 99.9 + %) served as feedstock where the inlet molar flow rate was in the overall range of 8.9×10^{-3}–4.1×10^{-2} h^{-1} and the reaction temperature was maintained at 343 K. The hydrogen partial pressure was varied in the range 0.17–0.94 atm by dilution in helium and all kinetic measurements were made with hydrogen in at least fivefold excess relative to stoichiometric quantities. In a series of blank experiments, passage of 2-butanone in a stream of hydrogen through the empty reactor, i.e., in the absence of the catalyst, did not result in any detectable conversion within the experimental regime that was employed for the catalytic reactions. The catalytic measurements were made at an overall gas space velocity of 560–4500 h^{-1} and, in order to test adherence to pseudo-first-order kinetic behaviour, the W/Q values were varied in the range 0.6–0.1 g cm^{-3} h where W is the weight of activated catalyst and Q is the 2-butanone volumetric feed rate. The reactor effluent was frozen in a liquid nitrogen trap for subsequent analysis which was made using an AI Cambridge GC94 chromatograph equipped with a split/splitless injector and a flame ionisation detector, employing a G-TA 20 m $\times$ 0.25 mm Chiraldex capillary column (Astec) which facilitated direct quantitative analysis of the optically active product mixtures. Data acquisition and analysis were performed using the JCL 6000

Table 1
Physical characteristics of the catalyst precursors and activated material

Sample	Preparation	% w/w Ni	% w/w H_2O	D^a (%)	d^b (nm)
Ni/SiO_2-A	precipitation/deposition	1.5	0.6	73	1.4
Ni/SiO_2-B	precipitation/deposition	6.1	1.2	54	1.9
Ni/SiO_2-C	precipitation/deposition	11.9	2.0	40	2.5
Ni/SiO_2-D	precipitation/deposition	15.2	3.6	33	3.1
Ni/SiO_2-E	precipitation/deposition	20.3	4.5	27	3.7
Ni/SiO_2-F	impregnation	11.6	8.0	17	5.9
Ni/Na-Y	ion exchange	2.2	26.6	3	39

[a]Ni dispersion.
[b]Average Ni particle diameter.

(for Windows) chromatography data system where quantitative analysis was based on relative peak area with acetone as solvent; reproducibility was better than $\pm 0.4\%$ and the detection limit typically corresponded to a feedstock conversion less than 0.5 mol%. Peak area was converted to mole fraction using detailed (at least 20-point) calibration plots involving combinations of 2-butanone, (*R*)-(−)-2-butanol and (*S*)-(+)-2-butanol (Aldrich, 99%). The fractional conversion (x) of the 2-butanone feedstock is defined as

$$x = \frac{[\text{2-butanone}]_i - [\text{2-butanone}]_o}{[\text{2-butanone}]_i} \quad (1)$$

where [ ] denotes concentration and the subscripts i and o refer to 2-butanone entering and exiting the reactor, respectively. Enantioselectivity is expressed in terms of enantiomeric excess (ee) which, in the case of an excess of (*S*)-(+)-2-butanol, is given by

$$\%\text{ee} = \frac{[(S)\text{-}(+)\text{-2-butanol}] - [(R)\text{-}(-)\text{-2-butanol}]}{[(S)\text{-}(+)\text{-2-butanol}] + [(R)\text{-}(-)\text{-2-butanol}]} \times 100. \quad (2)$$

At the end of each catalytic run, the catalyst was normally heated in flowing dry hydrogen (100 $cm^3\ min^{-1}$) at 5 K min^{-1} to 673 K which was maintained for at least 12 h; the effect of varying this regeneration temperature from 343 to 673 K was also examined. In many cases the reaction was repeated under identical conditions where product composition was reproducible to better than $\pm 6\%$. All the chemicals used were thoroughly purged with helium before use.

3. Results and discussion

3.1. Non-selective hydrogenation

The hydrogenation of 2-butanone over each unmodified catalyst yielded an essentially racemic 2-butanol product where the ee (in terms of the *S* form) was always less than 4%. The pertinent physical characteristics of the catalyst precursors and activated materials are given in Table 1. In every instance, the fractional conversion of the 2-butanone feed declined with time-on-stream, as is illustrated in Fig. 1 for three representative volumetric feed rates. It is immediately evident that conversion is time dependent and, while there was a decided drop in activity (typically over the initial 5-h period), a

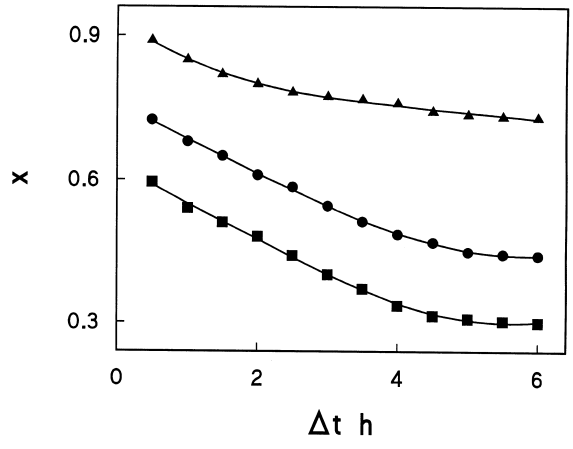

Fig. 1. Variation with time-on-stream of the fractional conversion (x) of 2-butanone at 343 K over Ni/SiO_2-C with varying volumetric feed rate, Q, of: (▲) 1.2, (●) 2.2 and (■) 3.6 $cm^3\ h^{-1}$.

steady state conversion was ultimately achieved and maintained. This steady state level of conversion is used, from this point on, as the basis for comparison of the effects on catalytic activity of altering either the process conditions or the nature of the catalyst. A drop in activity with time is frequently observed with reactors that operate in a continuous-flow mode where the activity loss is normally ascribed to a poisoning by carbonaceous residues [25] and the transition metals, notably Fe, Co and Ni, are particularly prone to carbon deposition [26]. Moreover, Szollosi and Bartok [11] likewise observed a decline in activity in the gas phase conversion of 2-butanone over MgO. The loss of activity in this study was reversible in that a prolonged (>12 h) catalyst regeneration in a flow of dry hydrogen at elevated temperatures served, upon returning to the same reaction temperature, to deliver an equivalent level of hydrogenation activity to that which was generated using the freshly activated catalyst. A full restoration of the initial activity however required a regeneration temperature in excess of 573 K and the post-regeneration fractional conversions decreased with a decreasing regeneration temperature, as is illustrated in Fig. 2. The possibility of thermodynamic limitations was considered by estimating the pertinent gas phase constants using the NIST database [27]. The resultant calculations yielded an equilibrium

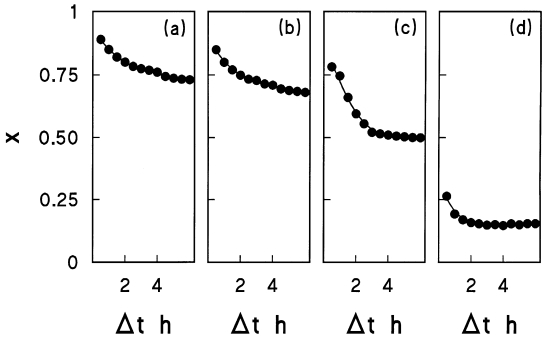

Fig. 2. Time-on-stream profiles for the fractional conversion (x) of 2-butanone at 343 K after (a) catalyst regeneration at 673 K, (b) catalyst regeneration at 573 K, (c) catalyst regeneration at 423 K and (d) catalyst regeneration at 343 K.

constant (K_p) in the form of a temperature-dependence ($300 \le T \le 1000$ K)

$$\log K_p = \frac{(P_{2\text{-butanol}})}{(P_{2\text{-butanone}})(P_{H_2})} = -5.7 + \frac{2822}{T}. \quad (3)$$

Within the experimental regime used in this study, hydrogenation can be considered irreversible where the above relationship predicts complete conversion of the 2-butanone reactant under equilibrium conditions. The experimental catalytic conversions are all below the equilibrium values and the various responses to alterations in process variables can be positively attributed to surface reaction phenomena.

Hydrogenation kinetics can be approximated by a pseudo-first-order treatment which is tested, in this application, by integrating the design equation for a plug flow reactor. The pertinent design equation [24] for a pseudo-first-order reaction is

$$\frac{W}{F} = \frac{1}{k[\text{2-butanone}]_i} \int_0^x \frac{dx}{1-x} \quad (4)$$

where F is the molar flow rate and k is the pseudo-first-order rate constant and this takes the form

$$\ln\left(\frac{1}{1-x}\right) = k\frac{[\text{2-butanone}]_i W}{F} = k\frac{W}{Q} \quad (5)$$

where Q is the volumetric flow rate to the reactor. A pseudo-first-order rate-dependence yields a linear dependence of $\ln(1/1-x)$ on W/Q as is revealed in Fig. 3 for three representative Ni/SiO_2 catalysts. A least-squares fit, forced to go through the origin, was then used to determine the rate constant which increased in magnitude in the order Ni/SiO_2-B (1.8 $cm^3\ g^{-1}\ h^{-1}$) < Ni/SiO_2-D (2.3 $cm^3\ g^{-1}\ h^{-1}$) < Ni/SiO_2-C (3.0 $cm^3\ g^{-1}\ h^{-1}$). The possible involvement of structure sensitivity was probed by relating the experimentally determined pseudo-first-order rate constant to catalyst structure and extracting a specific rate which takes

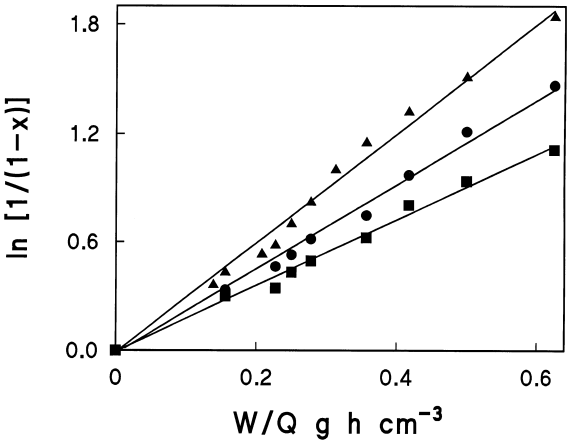

Fig. 3. Pseudo-first-order relationships for the hydrogenation of 2-butanone at 343 K over (■) Ni/SiO_2-B, (▲) Ni/SiO_2-C and (●) Ni/SiO_2-D.

account of the exposed nickel metal phase. The variation of the hydrogenation rate constant (per unit nickel area) with nickel particle diameter, taking an average area of 0.0633 nm^2 per surface nickel atom [28], is illustrated in Fig. 4 for the precipitation/deposition and impregnated nickel systems. There is a clear increase in rate on increasing the nickel particle size from 1 to 3 nm with a discernible loss of activity for larger supported nickel particles. The nickel particle sizes considered in this study largely fall within the so-called mitohedrical [29] or mesoscopic [30] region wherein catalytic reactivity can show a critical dependence on morphology. The observed antipathetic structure sensitivity with larger particles having higher activity than smaller ones leading to an intermediate size exhibiting an optimum specific activity has been established for a number reactions promoted using supported nickel catalysts [31]. In our nickel systems, the underlying pattern appears to extend to different catalyst preparative routes and an optimum nickel particle size of ca. 3 nm emerges. The catalysts prepared by deposition/precipitation are characterised by a narrower particle size distribution and stronger metal/support interactions than is the case for the impregnated precursor [21]. The relationship plotted in Fig. 4 supports the existence of some form of ensemble effect which may take the form of the (electronic/dynamic) optimum arrangement of atoms located on the principal crystal faces of the nickel particles. Dispersion and morphology of metal particles can, however, have a large effect on carbon deposition [26] and the observed variations in activity with metal particle size could conceivably be due to different degrees of coking or catalyst deactivation. In order to verify or discount this effect, the raw conversion vs. time profiles were fitted (correlation coefficient > 0.99), in every instance, to an empirical relationship of the form

$$x = x_{\text{initial}} \exp(-\alpha \Delta t) \quad (6)$$

where the coefficient α can be considered to reflect the time dependency of the fractional conversion and serves as a measure of the degree of short term deactivation. The values of α, at three representative 2-butanone volumetric feed rates are recorded in Table 2 for each Ni/SiO_2 catalyst. While the ''decay coefficient'' increased in magnitude at lower feed rates, indicative of a greater relative influence of time on activity, there is no discernible trend among the range of nickel-loaded silica samples and the extent of deactivation was essentially

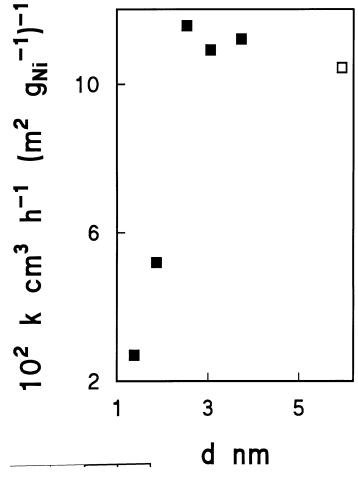

Fig. 4. Variation of the hydrogenation rate constant per unit nickel area at 343 K with nickel crystallite size over Ni/SiO_2 prepared by homogeneous precipitation/deposition (solid symbols) and impregnation (open symbol).

Table 2
Effect of the volumetric 2-butanone feed rate (Q) on the activity decay coefficient at 343 K for each Ni/SiO_2 catalyst

Catalyst	α (h^{-1})		
	$Q = 1.2$ $cm^3\ h^{-1}$	$Q = 2.2$ $cm^3\ h^{-1}$	$Q = 3.6$ $cm^3\ h^{-1}$
Ni/SiO_2-A	0.80	0.72	0.64
Ni/SiO_2-B	0.85	0.70	0.60
Ni/SiO_2-C	0.87	0.75	0.63
Ni/SiO_2-D	0.86	0.77	0.66
Ni/SiO_2-E	0.90	0.73	0.60
Ni/SiO_2-F	0.82	0.76	0.68

the same for each catalyst. The possible contribution of a surface poisoning in determining the observed structure sensitivity can therefore be discounted. The effect of varying the hydrogen partial pressure on activity was also considered and, as is evident from the results presented in Fig. 5, a decrease in the hydrogen/2-butanone pressure ratio below ca. 5 was accompanied by a drop in conversion. Catalyst deactivation was however more dominant for a fixed volumetric feed rate of 2-butanone at lower hydrogen partial pressures, i.e., α increasing (taking the data presented in Fig. 5) from 0.8 h^{-1} at 0.88 atm to 1.2 h^{-1} at 0.13 atm. An increase in the hydrogen pressure must serve to limit the extent of coke deposition and, in effect, clean the surface of the catalyst.

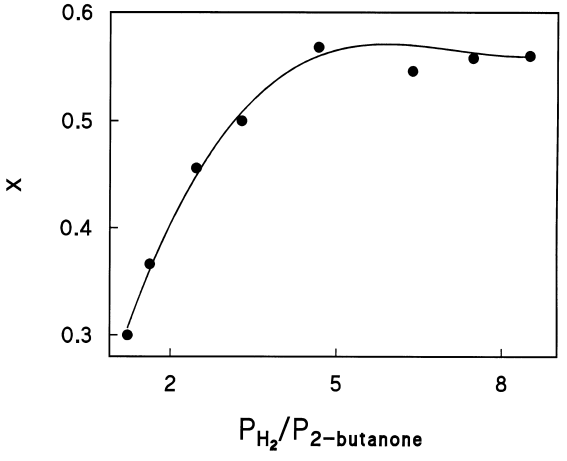

Fig. 5. Fractional conversion of 2-butanone (x) over Ni/SiO_2-C at 343 K as a function of hydrogen/2-butanone partial pressure ratios: $Q = 1.8$ $cm^3\ h^{-1}$.

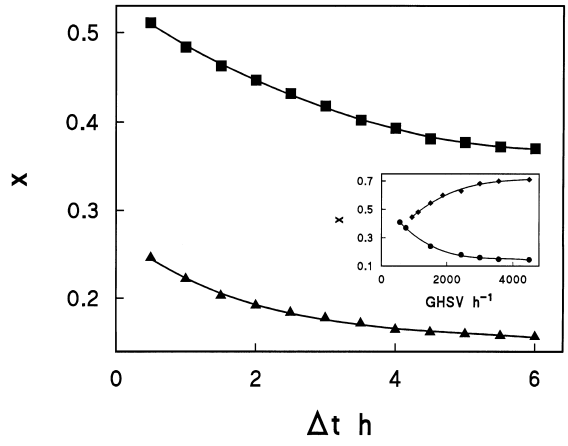

Fig. 6. Variation of fractional 2-butanone conversion (x) with time-on-stream over Ni/Na-Y at (▲) 413 K and (■) 483 K at $Q = 0.4$ $cm^3\ h^{-1}$ and $P_{H_2}/P_{2\text{-butanone}} = 11.2$. Inset: Effect of varying the gas hourly space velocity (GHSV) on the fractional conversion of 2-butanone over Ni/SiO_2-C at 343 K ((♦) $Q = 1.6$ $cm^3\ h^{-1}$) and Ni/Na-Y at 483 K ((●) $Q = 0.4$ $cm^3\ h^{-1}$).

Hydrogenation of 2-butanone over the nickel exchanged Y zeolite again generated a racemic product mixture. Under the same experimental conditions employed for the Ni/SiO_2-promoted reaction, the freshly activated Ni/Na-Y sample did not generate any measurable quantities of 2-butanol in the product stream and the reaction temperature had to be elevated from 343 to 383 K before any level of hydrogenation could be detected. Given this divergence from the behaviour observed for all the Ni/SiO_2 catalysts, the hydrogenation of 2-butanone certainly exhibits an appreciable degree of structure sensitivity. Hydrogenation over Ni/Na-Y was accompanied by a more marked loss of activity with time-on-stream as is revealed in Fig. 6 for two representative sets of process conditions. Moreover, regeneration in flowing hydrogen at 673 K did not fully restore the original levels of catalytic activity and after three cycles of reaction/regeneration the zeolite invariably exhibited only trace levels of 2-butanone conversion, i.e., $x < 0.03$. The Linde molecular sieve LZ-

52Y used in this study can be classified as a large pore aluminosilicate where access to the intracrystalline supercage metal sites is via 0.7–0.8 nm and 0.20–0.25 nm pore openings. Reduction of the nickel exchanged Na-Y zeolite generated a nickel metal phase which was characterised by a wide particle size distribution with particle growth resulting in the formation of larger metal particles on the external surface [22,32]. There is however an appreciable smaller particle component accommodated within the zeolite pore structure that serves to promote hydrogenation. The observed loss of activity can be ascribed to a pore blocking effect where the internal sites become occluded and the coke deposits are not effectively removed by a high-temperature treatment in flowing hydrogen. Such an effect has been well-established and reported for closely related zeolite catalytic systems [33,34]. The effect of varying the GHSV produced opposite effects on the degree of conversion over Ni/SiO_2 and Ni/Na-Y, as is illustrated in the inset to Fig. 6. An increase in GHSV from 940 to 3000 h^{-1} was accompanied by an increase in conversion over Ni/SiO_2-C, indicative of a higher turnover of reactant at lower contact times. The reverse was the case for Ni/Na-Y which can be taken to be diagnostic of a pore diffusion-controlled reaction.

3.2. Enantioselective hydrogenation

Treatment of each activated Ni/SiO_2 sample with the (*S*)-form of tartaric acid, glutamic acid and valine invariably generated (*S*)-(+)-2-butanol as the preferred product, albeit to varying degrees. Replacement of the modifier by its antipode generated roughly equivalent optical yields but with a reversal of sign while optically inactive *meso*-tartaric acid was found to deliver consistently a racemic product, i.e., ee < 3%. The in situ modification had little effect on product composition where activity was essentially the same as that recorded for the unmodified catalyst and only a minor degree of enantiodifferentiation was introduced. Representative catalytic data are included in Table 3 to illustrate the essentially invariant nature of activity/selectivity with or without the in situ treatment. There was a discernible increase in enantioselectivity at lower space velocities which is indicative of an enhancement at high contact times but the ee values that were generated did not exceed 8%. Performing the modification in situ did not generate an active phase that exhibited any marked enantiodifferentiation with respect to the conversion of a continuous flow of the prochiral feedstock. The ex situ treatment, however, resulted in markedly higher selectivities, as presented in Table 4. The degree of both activity and enantioselectivity were strongly effected by the concentration of the tartaric acid modifier and, over the range of concentrations employed (0.004–0.016 mol dm^{-3}), ee was observed to pass through a maximum value of 31%. Increasing the initial modifier concentration resulted in higher tartaric acid

Table 3
Effect of in situ modification of Ni/SiO_2-C with L-tartaric acid, L-valine and L-glutamic acid on the fractional conversion of 2-butanone (*x*) and ee

Treatment	$Q = 1.4$ cm^3 h^{-1}		$Q = 2.4$ cm^3 h^{-1}	
	x	ee (%)	*x*	ee (%)
No modification	0.53	1.8	0.30	3.0
+ L-tartaric acid	0.55	6.0	0.27	6.8
+ L-valine	0.46	5.2	0.29	4.4
+ L-glutamic acid	0.50	5.5	0.26	5.4

Table 4
Effect of ex situ modification of Ni/SiO_2-C, with varying concentrations of L-tartaric acid in methanol, on tartaric acid uptake (*N*), degree of nickel leaching and the ultimate fractional conversion of 2-butanone (*x*) and ee; $Q = 1.8$ cm^3 h^{-1}

[Tartaric acid] (mol dm^{-3})	Ni leached (ppm)	10^{19} *N*[a] (g^{-1})	*x*	ee (%)
–	–	–	0.56	< 1
4×10^{-3}	11	1.9	0.60	14
8×10^{-3}	23	3.2	0.63	31
12×10^{-3}	25	3.3	0.26	10
16×10^{-3}	35	3.8	0.10	4

[a] Number of tartaric acid molecules retained per gram of catalyst.

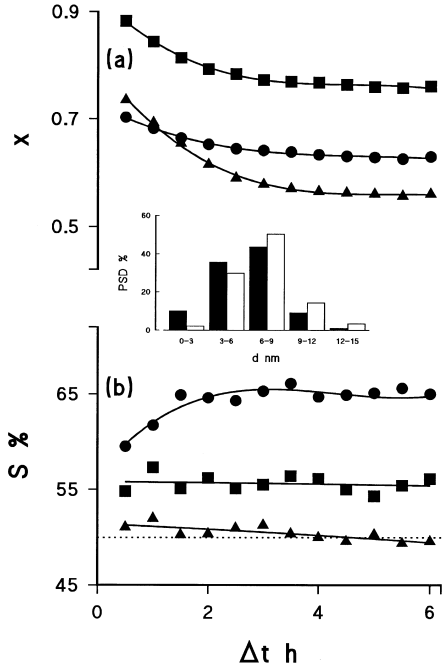

Fig. 7. Variation with time-on-stream of (a) the fractional 2-butanone conversion (x) and (b) selectivity with respect to (S)-(+)-2-butanol over a freshly activated Ni/SiO_2-C (▲), Ni/SiO_2-C directly after ex situ modification in an 8.2×10^{-3} mol dm^{-3} methanolic tartaric acid (●) and the modified Ni/SiO_2-C after hydrogen regeneration at 673 K (■); the dotted line represents a racemic product mixture. Inset: Nickel particle size distribution (PSD) in the freshly activated (solid bars) and modified/regenerated (open bars) Ni/SiO_2-F.

uptakes by the solid as has been noted elsewhere [12,14]. Tartaric acid treatment is known to be a corrosive process where some of the surface nickel metal can be leached into solution [12,14,35]. In this study, while the concentration of nickel in the post-modifier solution increased with increasing modifier concentration, the degree of leaching was not appreciable and represents less than 3% of the nickel content. Under the optimum modification conditions, the fractional conversion was higher than that delivered by the unmodified catalyst and the degree of short-term deactivation was lower, as is evident from the profiles presented in Fig.7(a). Modification with tartaric acid not only induced enantiodifferentiation but also raised the degree of hydrogenation activity. A similar effect has been noted in the liquid phase hydrogenation of a carbonyl functionality [36] where the higher reaction rates over modified surfaces were attributed to modifier/reactant interaction(s) which serve(s) to polarise the C═O bond, rendering it more susceptible to hydrogen attack. A regeneration of the tartaric acid-modified catalyst in hydrogen at 673 K produced, on returning to the same reaction temperature, a more active catalyst. This modification/regeneration step was however accompanied by a shift in the average nickel particle size to a higher value, as illustrated in the inset to Fig. 7, which may account for the elevated conversions in this structure sensitive reaction system. However, the high-temperature treatment resulted in a marked loss of enantioselectivity (Fig. 7(b)) and the initial induction period observed for the freshly modified sample wherein selectivity increased with time before attaining a steady state value, was no longer evident. The disappearance of enantioselectivity is no doubt due to a temperature induced desorption of the tartaric acid modifier but some residual (greater than the unmodified system) enantiodifferentiation was nevertheless retained.

4. Conclusions

In the gas phase continuous catalytic hydrogenation of 2-butanone in a plug flow reactor, the data presented in this paper support the following conclusions.

(i) Unmodified nickel/silica and nickel/zeolite catalysts, operating in the absence of thermodynamic limitations, generate a racemic product where short term conversion is subject to a decline with time-on-stream. This loss of activity is reversible in the former case and a regeneration in hydrogen at elevated temperatures restores activity but is irreversible in zeolite-promoted catalysis.

(ii) The reaction is structure sensitive and exhibits an increase in specific activity with an increase in the average nickel particle size leading to an optimum supported particle diameter

of ca. 3 nm, an effect that is independent of catalyst deactivation.

(iii) Pseudo-first-order kinetics adequately represent the variation of conversion with increasing volumetric feed rate over Ni/SiO_2 where, at a fixed inlet feed rate, conversion decreased (and the degree of deactivation increased) at hydrogen/2-butanone partial pressure ratios below ca. 5. An increase in GHSV to ca. 3000 h^{-1} both raises and lowers conversion over Ni/SiO_2 and Ni/Na-Y, respectively.

(iv) In situ modification of Ni/SiO_2 with L-tartaric acid, L-valine and L-glutamic acid has a negligible effect on selectivity/activity. An ex situ liquid phase treatment with methanolic solutions of L-tartaric acid results in a preferential formation of (*S*)-(+)-2-butanol where the degree of enantioselectivity is dependent on tartaric acid concentration. A maximum ee of 31% has been achieved and this is accompanied by a higher fractional conversion than that recorded for the unmodified sample. Heating this sample to 673 K in hydrogen results in a marked loss of enantioselectivity but serves to further increase activity, presumably due to a favourable shift in the particle size distribution.

Acknowledgements

This work was supported by a grant (No. 17576) from the Royal Society.

References

[1] A.N. Collins, G.N. Sheldrake, J. Cosby, Chirality Ind. 1 (1995) Wiley, New York.
[2] I.A. Satinder, Chiral Sep. (1997) American Chemical Society, Washington, DC.
[3] J. Jacques, A. Collect, S.H. Wilen, Enantiomers, Racemates and Resolutions, Wiley, New York, 1981.
[4] G. Procter, Asymmetric Synthesis, Oxford Univ. Press, Oxford, 1996.
[5] J.E. Bailey, D.F. Ollis, Biochemical Engineering Fundamentals, McGraw-Hill, Singapore, 1997.
[6] H. Brunner, W. Zettlmeier, Handbook of Enantioselective Catalysis with Transition Metal Compounds, VCH Verlagsgesellschaft, Weinheim, 1993.
[7] Y. Izumi, Adv. Catal. 12 (1983) 215.
[8] H.U. Blaser, M. Muller, Tetrahedron: Asymmetry 2 (1991) 843.
[9] M. Hernandez, P. Kalck, J. Mol. Catal. A: Chem. 116 (1997) 131.
[10] Y. Yoshikawa, Y. Iwasawa, J. Mol. Catal. A: Chem. 100 (1995) 115.
[11] G. Szollosi, M. Bartok, Appl. Catal., A 169 (1998) 263.
[12] M.A. Keane, Catal. Lett. 19 (1993) 197.
[13] M.A. Keane, Langmuir 13 (1997) 41.
[14] M.A. Keane, G. Webb, J. Catal. 136 (1992) 1.
[15] M.A. Keane, G. Webb, J. Mol. Catal. 73 (1992) 91.
[16] M.A. Keane, Langmuir 10 (1994) 4560.
[17] T. Osawa, T. Harada, A. Tai, J. Catal. 121 (1990) 7.
[18] T. Osawa, Chem. Lett. (1986) 1609.
[19] T. Harada, T. Osawa, G. Jannes, V. Dubois (Eds.), Chiral React. Heterog. Catal. (1995) 83, Plenum, New York.
[20] E. Keinan, E.K. Hafeli, K.K. Steh, R. Lamed, J. Am. Chem. Soc. 108 (1986) 162.
[21] M.A. Keane, Can. J. Chem. 72 (1994) 372.
[22] B. Coughlan, M.A. Keane, Zeolites 11 (1991) 2.
[23] B. Coughlan, M.A. Keane, J. Catal. 123 (1990) 364.
[24] O. Levenspeil, in: Chemical Reaction Engineering, 2nd edn., Wiley, New York, 1972, p. 97.
[25] G.C. Bond, Chem. Soc. Rev. 20 (1991) 441.
[26] G.C. Bond, Appl. Catal., A 149 (1997) 3.
[27] S.G. Lias, J.F. Liebman, R.D. Levin, S.A. Kafafi, NIST Standard Reference Database 25, Structure and Properties, Version 2.01, January 1994.
[28] M. Nele, A. Vidal, D.L. Bhering, J.C. Pinto, V.M.M. Salim, Appl. Catal., A 178 (1999) 177.
[29] O.M. Poltorak, V.S. Boronin, Russ. J. Phys. Chem. 40 (1966) 1436.
[30] H. Müller, C. Opitz, L. Skala, J. Mol. Catal. 54 (1989) 389.
[31] M. Che, C.O. Bennett, Adv. Catal. 36 (1989) 55.
[32] M.A. Keane, Zeolites 19 (1993) 14.
[33] B. Coughlan, M.A. Keane, J. Mol. Catal. 71 (1992) 93.
[34] M.A. Keane, Ind. J. Technol. 30 (1992) 51.
[35] M.A. Keane, G. Webb, J. Chem. Soc., Chem. Commun. (1991) 1619.
[36] M.A. Keane, J. Chem. Soc., Faraday Trans. 93 (1997) 2001.